Manipulating magnetic anisotropies of Co/MgO(001) ultrathin films via oblique deposition*

Syed Sheraz Ahmad, Wei He(何为), Jin Tang(汤进), Yong Sheng Zhang(张永圣), Bo Hu(胡泊), Jun Ye(叶军), Qeemat Gul, Xiang-Qun Zhang(张向群), and Zhao-Hua Cheng(成昭华)†

State Key Laboratory of Magnetism and Beijing National Laboratory for Condensed Matter Physics, Institute of Physics, Chinese Academy of Sciences, Beijing 100190, *China*

(Received 23 May 2016; revised manuscript received 27 June 2016; published online 2 August 2016)

We present a systematic investigation of magnetic anisotropy induced by oblique deposition of Co thin films on MgO (001) substrates by molecular beam epitaxy at different deposition angles, i.e., 0°, 30°, 45°, 60°, and 75° with respect to the surface normal. Low energy electron diffraction (LEED), surface magneto–optical Kerr effect (SMOKE), and anisotropic magnetoresistance (AMR) setups were employed to investigate the magnetic properties of cobalt films. The values of in-plane uniaxial magnetic anisotropy (UMA) constant K_u and four-fold magnetocrystalline anisotropy constant K_1 were derived from magnetic torque curves on the base of AMR results. It was found that the value of K_u increases with increasing deposition angle with respect to the surface normal, while the value of K_1 remains almost constant for all the samples. Furthermore, by using MOKE results, the K_u values of the films deposited obliquely were also derived from the magnetization curves along hard axis. The results of AMR method were then compared with that of hard axis fitting method (coherent rotation) and found that both methods have almost identical values of UMA constant for each sample.

Keywords: magnetic anisotropy, oblique deposition, cobalt ultrathin film, anisotropic magnetoresistance

PACS: 75.30.Gw, 75.60.Jk, 75.70.Ak **DOI:** 10.1088/1674-1056/25/9/097501

1. Introduction

The surface morphology and microstructure of thin films have a direct impact on the magnetic anisotropy. There are two main sources of magnetic anisotropy: one is spin–orbit interaction, which causes magnetocrystalline anisotropy (MCA) and the other is dipolar interaction, which causes shape anisotropy.[1,2] The study and tuning of anisotropy in magnetic thin films have attracted much attention because of its applications in data storage devices and magnetoresistive devices. To improve the storage capability of these devices, a highly uniaxial magnetic anisotropy (UMA) is required. Especially, in magnetoresistive random access memory and head assemblies of the hard drivers, in-plane UMA is required.[3] Different methods, such as oblique deposition[4] applying a magnetic field during deposition,[5] increasing the substrate temperature[6] and post-annealing (annealing in the presence of the magnetic field), have been adopted to induce the magnetic anisotropy.[7] The effect of oblique deposition on the magnetic anisotropy has long been established.[8,9] It is known that shadowing and steering effect, in the case of oblique deposition, leads to elongated grain structure or ripples. These elongated grain structures and ripples induce in-plane UMA.[10]

Different techniques such as ferromagnetic resonance (FMR)[11] magnetic hysteresis loop measurement, torque measurement[12] rotational magneto-optic Kerr effect (ROTMOKE)[13] magnetic transverse biased initial inverse susceptibility and torque (TBIIST)[14] have been adapted to manipulate the magnetic anisotropy. It is known for ultra-thin films that the coherent domain rotation magnetization reversal does not always happen, particularly when the applied field is lower than the saturation field. Therefore, it is difficult to distinguish the detailed information regarding the magnetic anisotropy accurately from the magnetization hysteresis loops. On the other hand, magnetotransport technique has been suggested to be a powerful technique for magnetic anisotropy in thin single layer films by AMR[15–20] This can be acquired by applying an appropriately large field to ensure a true single-domain rotation.

Co/MgO system is the point of our interest because of its application in magnetoelectronics. A lot of studies have been done in the past on the growth behavior and the structure of Co film on the MgO (001) substrate. However, magnetic properties of Co film on MgO (001) have not been studied in detail. In this paper the magnetic anisotropy constants of Co ultrathin films obliquely deposited on MgO (001) substrates have been determined by using MOKE and AMR techniques.

*Project supported by the Chinese Academy of Sciences–The World Academy of Sciences (CAS–TWAS) Fellowship Program, the National Basic Research Program of China (Grant Nos. 2015CB921403 and 2012CB933102), and the National Natural Science Foundation of China (Grant Nos. 51427801, 11374350, and 11274361).

†Corresponding author. E-mail: zhcheng@iphy.ac.cn

© 2016 Chinese Physical Society and IOP Publishing Ltd

2. Experimental details

Experiments were performed in the molecular beam epitaxy (MBE) system with a base pressure of 2.0×10^{-10} mbar. Crystalline polished MgO (001) substrates were used for the deposition of Co films. As the surface of the commercially available MgO substrate is contaminated by water and carbon, the substrates were first annealed in the ultra-high vacuum chamber at 700 °C for about 2 h to remove the carbon contamination. After annealing the substrates, low energy electron diffraction (LEED) pattern was studied using the LEED system to confirm the surface cleanliness. Ultrathin Co films were then deposited at room temperature and at different angles with respect to surface normal using an electron beam evaporator. The thicknesses of all the five samples were kept constant (9 ML) that were achieved by increasing the growth time with increasing the deposition angle. Before taking out the samples from the vacuum chamber, copper (Cu) films of about 25 ML were caped to avoid the oxidation of the samples. The corresponding magnetic hysteresis loops were measured by MOKE with azimuthal rotation to measure the oblique deposition-induced uniaxial anisotropy. The angular dependence AMR measurement setup with a standard four-point method was used to determine the values of magnetic anisotropy constants at room temperature for obliquely deposited Co thin films on MgO (001) substrates.

3. Results and discussion

Figure 1(a) shows the schematic configuration of the sample and figure 1(b) shows the LEED pattern of the MgO (001) substrate. The angular dependent normalized remanence loops obtained from the longitudinal MOKE data, for all the samples, having the same thickness (9 ML) deposited at different angles with respect to the surface normal are shown in Fig. 2. It is obvious that the angular dependence of the normalized remanence of the film normally deposited exhibits weak magnetocrystalline anisotropy (MCA) with four-fold symmetry. But the samples deposited obliquely with different deposition angles with respect to the surface normal exhibit UMA, as shown in Figs. 2(b)–2(e). It is known that the oblique deposition leads to elongated grain structures or ripples. These elongated grain structures or ripples induce in-plane (UMA).[10]

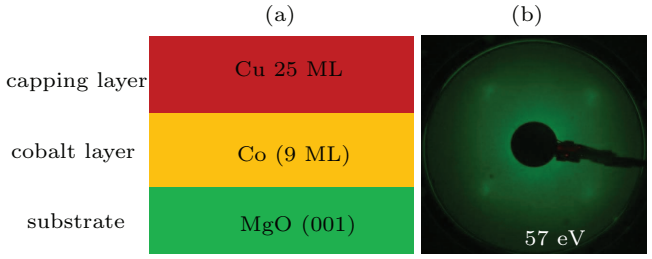


Fig. 1. (color online) (a) Schematic configuration of the sample, (b) the LEED pattern of MgO (001) substrate.

During the oblique deposition a self-shadowing effect takes place , resulting in the formation of grains in the plane of the film that is elongated perpendicular to the incident flux direction and with an aspect ratio increasing at a larger deposition angle. Therefore, the inhomogeneous distribution of the adatoms (roughness) occurs. This in-plane K_u with easy axis perpendicular to the incident flux direction is actually induced by the roughness due to the oblique deposition. Therefore, as the incidence angle increases the roughness is increased causing the increase in the magnitude of K_u,[2,3] as shown in Figs. 2(b)–2(e).

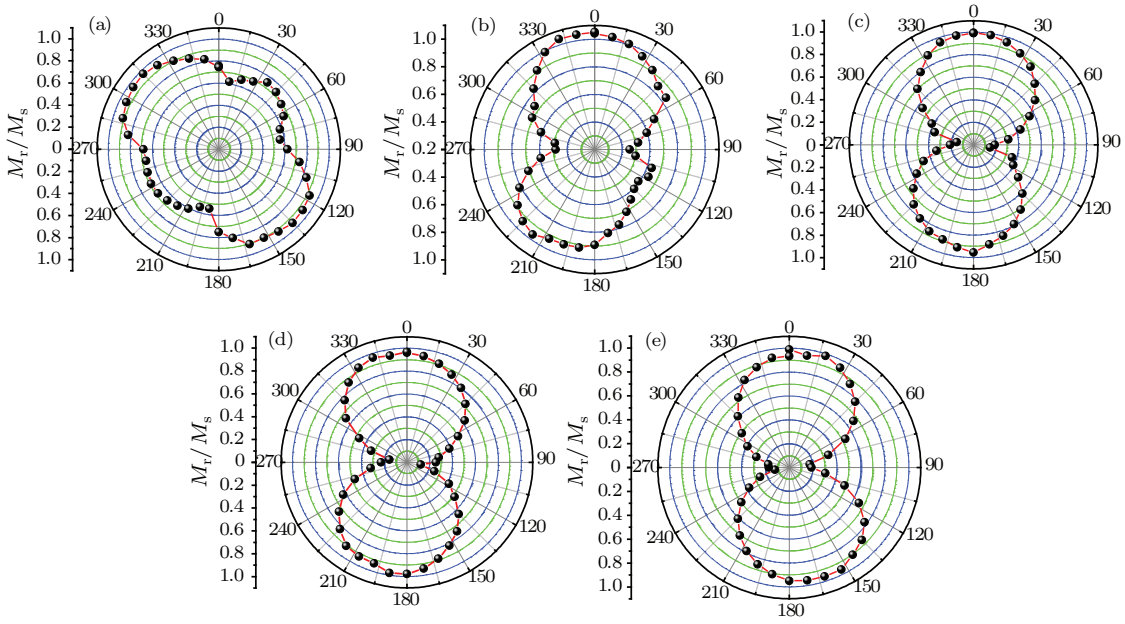


Fig. 2. (color online) Angular dependence of the normalized remanence (M_r/M_s) of 9-ML Co thin film on MgO (001) substrate at different deposition angles with respect to the surface normal. (a) 0°, (b) 30°, (c) 45°, (d) 60°, and (e) 75°.

We determined the values of the magnetic anisotropy constants for all of the samples from the torque curves using AMR measurements. The AMR can be expressed as

$$R_{xx}=R_{\perp}+(R_{\parallel}-R_{\perp})\cos^2\varphi_M, \tag{1}$$

where φ_M is the angle between the directions of the current flow and magnetization M, $R_{\parallel}$ is the resistance at $\varphi_M = 0°$ and $R_{\perp}$ is the resistance at $\varphi_M = 90°$. To ensure a true single domain rotation and eliminate the ordinary magnetoresistance effects, the externally applied magnetic fields are larger than the saturation field. The angular dependence of AMR curves of all the samples is shown in Fig. 3. It is clear that the AMR curves exhibit an oscillated behavior between maxima $R_{\perp}$ and minima $R_{\parallel}$. Here, two types of torques are acting on the magnetization M in the presence of external magnetic field. One is the torque due to the external magnetic field acting to rotate the magnetization in the direction of applied field H

$$L_H=\mu_0 M_s H\sin(\varphi_H-\varphi_M), \tag{2}$$

where μ_0 is the permeability of the free space and φ_H is the angle between the applied field and direction of current flow.

The second is the torque due to the crystal structure of the sample acting to rotate the magnetization towards the easy axis

$$L_k = K_u\sin 2\varphi_M + (K_1/2)\sin 4\varphi_M. \tag{3}$$

The first term is for UMA and the second term is for fourfold MCA. By comparing both torques, the normalized torque $l(\varphi_M) = L_k/\mu_0 M_s H = \sin(\varphi_H - \varphi_M)$ is introduced, so the normalized magnetic torque can be written as

$$l(\varphi_M) = \frac{\{K_u\sin 2\varphi_M + (K_1/2)\sin 4\varphi_M\}}{\mu_0 M_s H}. \tag{4}$$

The normalized magnetic torque curves for all samples are shown in Fig. 4. The AMR results are consistent with the MOKE results, i.e., the sample deposited with normal deposition exhibits MCA with weak fourfold symmetry as shown in Fig. 4(a). However, with the increase of the deposition angle, the UMA becomes stronger as shown in Figs. 4(b)–4(e).

The values of K_u were determined by fitting the normalized magnetic torque curves with Eq. (4). It is clear that the sample deposited at 0° with respect to the surface normal exhibits the lowest value of UMA $K_u = 5.8\times10^3$ J/m^3 with dominant fourfold MCA $K_1 = 6.9\times10^3$ J/m^3, while the sample deposited at 75° with respect to surface normal the UMA apparently levels into a maximum value of $K_u = 2.5\times10^4$ J/m^3.

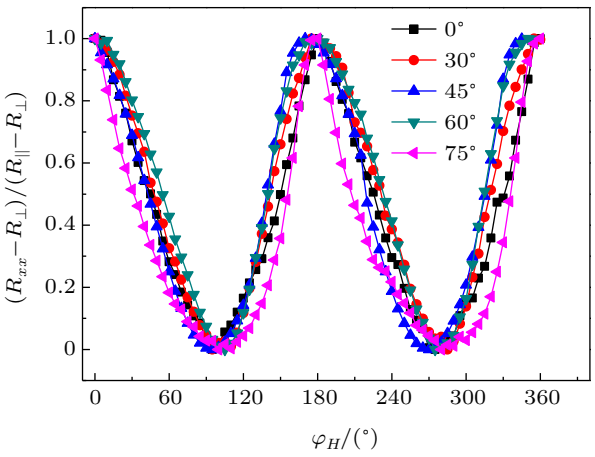


Fig. 3. (color online) The angular dependence of the in-plane AMR curves.

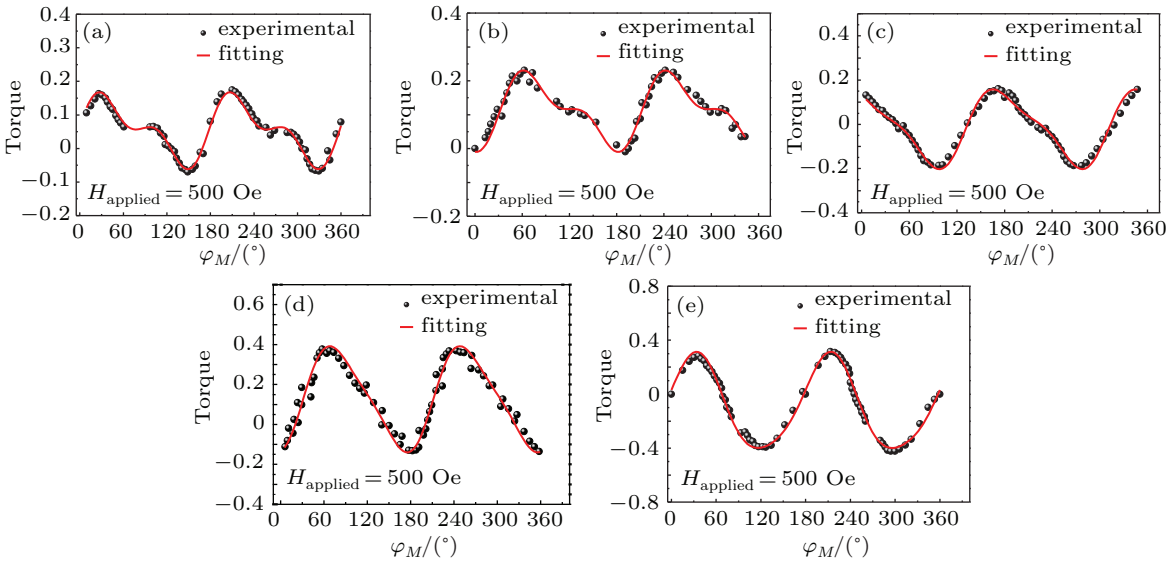


Fig. 4. (color online) The normalized magnetic torque curves of Co thin films on MgO (001) substrates at different deposition angles with respect to the surface normal. (a) 0°, (b) 30°, (c) 45°, (d) 60°, and (e) 75°.

The determined values of UMA constant (K_u) and MCA constant (K_1) for all the samples as a function of deposition angles are shown in Fig. 5(a). We can see that K_u shows an increasing curve while K_1 shows a constant behavior with the deposition angle. We note that by oblique deposition we can only induce UMA and could not alter the MCA. The values of K_1 and K_u are also displayed as a function of the applied magnetic field in Figs. 5(b) and 5(c). The magnetic anisotropy constants almost show an invariant behavior with respect to the applied field which are in good agreement with the results of Ye *et al.* for Fe/Si (001) films.[21]

Further, we have calculated the values of UMA for all samples deposited by oblique deposition at different angles, using MOKE data applying hard axis fitting method. Ignoring the relatively weak MCA, the total magnetic energy is given as

$$E = K_u \sin^2\theta - HM\cos(\varphi - \theta), \tag{5}$$

where φ and θ are the angles of the external applied magnetic field (H) and magnetization (M) with easy axis, respectively. The first term on the right side is UMA and the second term is Zeeman energy. Using Eq. (5), we can derive

$$K_u = \frac{H_a M_s}{2}, \tag{6}$$

where H_a is called as anisotropy field (the field at which the magnetization reaches to its saturation value). By fitting the hard axis loop of experimental data with Eq. (6), the value of UMA was deduced for each sample. The MH loops for the easy axis and hard axis fitting curves of all the samples are shown in Fig. 6. The sample deposited at 30° shows the

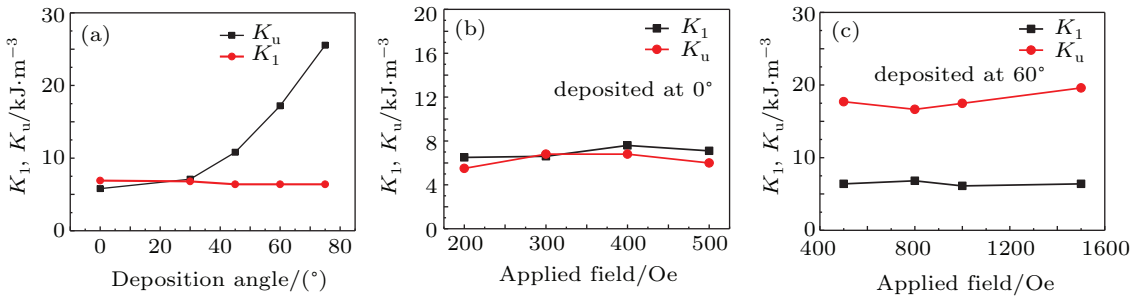


Fig. 5. (color online) UMA (K_u) and MCA (K_1) as functions of the deposition angle (a) and the applied field for normally deposited film (b) and 60° obliquely deposited film (c), respectively.

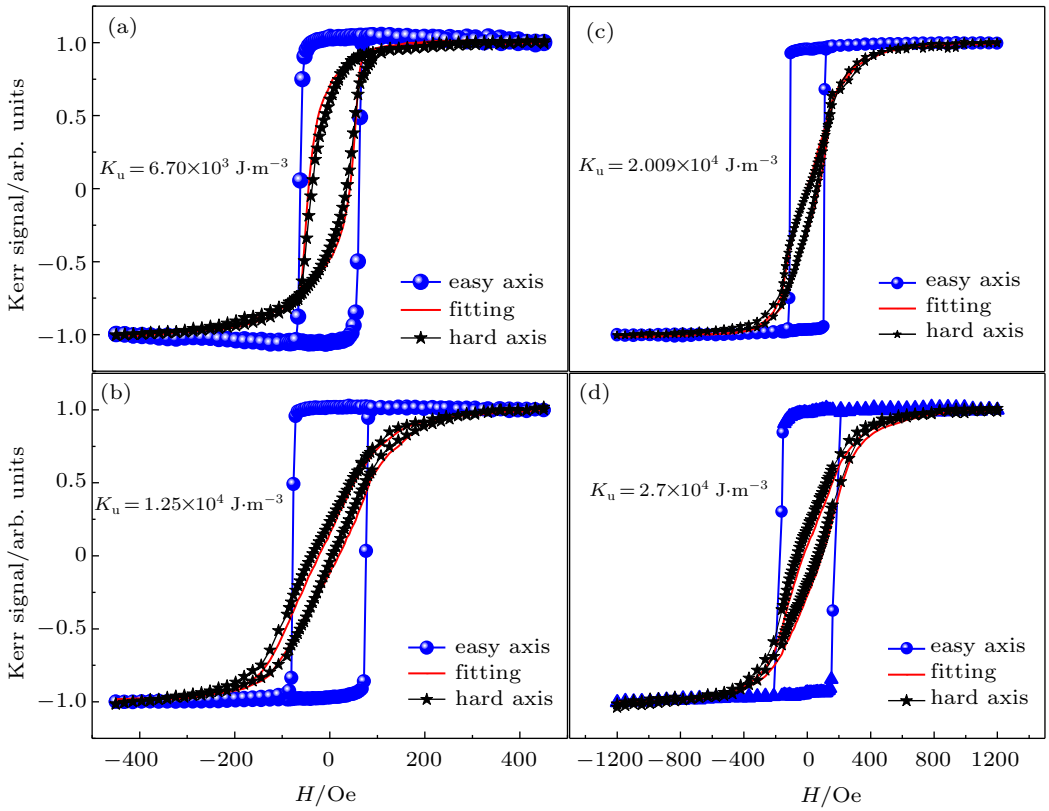


Fig. 6. (color online) Experimental and the fitting hysteresis loops. Typical in-plane magnetic hysteresis loops of the film deposited at different angles with respect to the surface normal. (a) 30°, (b) 45°, (c) 60°, and (d) 75°.

lowest value of $K_u = 6.70\times10^3$ J/m^3 and the sample deposited at 70° shows the maximum value of $K_u = 2.74\times10^4$ J/m^3. It is quite clear that the results of the hard axis fitting method (coherent rotation) and the results of the AMR method have almost identical values of K_u for each sample deposited obliquely. The values of K_u (as calculated by both methods) follow the same pattern with the deposition angle as shown in Fig. 7.

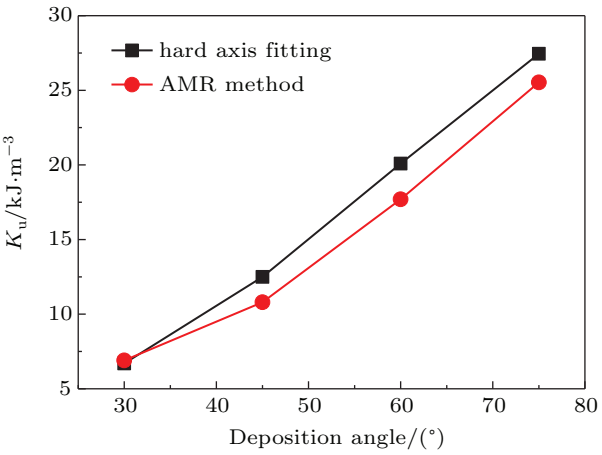


Fig. 7. (color online) Comparison of the values of UMA (K_u) determined by AMR method and hard axis fitting method.

4. Conclusion

In summary, the in-plane UMA K_u induced by oblique deposition shows an increasing behavior with the deposition angle while K_1 shows an invariant behavior. The values of MCA constant K_1 and UMA constant K_u exhibit almost a linear behavior with the applied field. The results of AMR method and MOKE have almost identical values of UMA for each sample.

References

[1] Zhao H W, Wu Y Z, Won C and Qiu Z Q 2004 *J. Appl. Phys.* **95** 7300
[2] Fang Y P, He W, Liu H L, Zhan Q F, Du H F, Wu Q, Yang H T, Zhang X Q and Cheng Z H 2010 *Appl. Phys. Lett.* **97** 22507
[3] Chowdhury N and Bedanta S 2014 *AIP Adv.* **4** 027104
[4] Smith D O, Cohen M S and Weiss J P 1960 *J. Appl. Phys.* **31** 1755
[5] Bedanta S, Eimuller T, Kleemann W, Rhensius J, Stromberg F, Amaladass E, Cardoso S and Freitas P P 2007 *Phys. Rev. Lett.* **98** 176601
[6] Pires M J M, Cotta A A C Martins M D, Silva A M A and Macedo W A A 2011 *J. Magn. Magn. Mater.* **323** 789
[7] Takahashi M and Kono T 1960 *J. Phys. Soc. Jpn.* **15** 936
[8] Knorr T G and Hoffman R W 1959 *Phys. Rev.* **113** 1039
[9] Hoshi Y, Suzuki E and Naoe M 1996 *J. Appl. Phys.* **79** 4945
[10] Madurga V, Vergara J and Favieres C 2004 *J. Magn. Magn. Mater.* **272–276** 1681
[11] Rezende S M, Moura J A S, De Aguiar F M and Schreiner W H 1994 *Phys. Rev. B* **49** 15105
[12] Yaegashi S, Kurihara T and Satoh K 1997 *J. Appl. Phys.* **81** 6303
[13] Mattheis R and Quednau G 1999 *J. Magn. Magn. Mater.* **205** 143
[14] Garreau G, Hajjar S, Bubendorff J L, Pirri C, Berling D, Mehdaoui A, Stephan R, Wetzel P, Zabrocki S, Gewinner G, Boukari S and Beaurepaire E 2005 *Phys. Rev. B* **71** 094430
[15] McGuire T R and Potter R I 1975 *IEEE Trans. Mag.* **11** 1018
[16] Dahlberg E D, Riggs K and Prinz G A 1988 *J. Appl. Phys.* **63** 4270
[17] Miller B H and Dahlberg E D 1996 *Appl. Phys. Lett.* **69** 3932
[18] Krivorotov I N, Leighton C, Nogues J, Schuller I K and Dahlberg E D 2002 *Phys. Rev. B* **65** 100402
[19] Cao W N, Li J, Chen G, Zhu J, Hu C R and Wu Y Z 2011 *Appl. Phys. Lett.* **98** 262506
[20] Li J, Jin E, Son H, Tan A, Cao W N, Hwang C and Qiu Z Q 2012 *Rev. Sci. Instrum.* **83** 033906
[21] Ye J, He W, Wu Q, Hu B, Tang J, Zhang X Q, Chen Z Y and Cheng Z H 2014 *Appl. Phys. Lett.* **105** 102406